AD-A183 718 SCATTERING PARAMETER TRANSIENT ANALYSIS OF TRANSMISSION LINES LOADED WITH.. (U) ILLINOIS UNIV AT URBANA ELECTROMAGNETIC COMMUNICATION LAB 1/1

UNCLASSIFIED J E SCHUTT-AINE ET AL. MAR 87 UIEC-EMC-87-2 F/G 9/1 NL

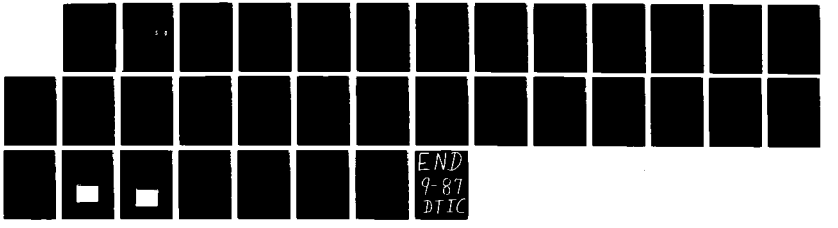

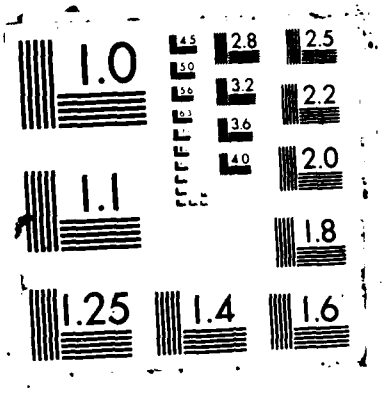
1.0
1.1
1.25
1.4
1.6
2.8
3.2
3.6
4.0
2.5
2.2
2.0
1.8

ELECTROMAGNETIC COMMUNICATION LABORATORY
TECHNICAL REPORT NO. 87-2

March 1987

SCATTERING PARAMETER TRANSIENT ANALYSIS OF TRANSMISSION LINES LOADED WITH NONLINEAR TERMINATIONS

J. E. Schutt-Aine

R. Mittra

Supported by

Department of the Navy
Office of Naval Research
Contract No. N00014-85-K0619

ELECTROMAGNETIC COMMUNICATION LABORATORY
DEPARTMENT OF ELECTRICAL AND COMPUTER ENGINEERING
UNIVERSITY OF ILLINOIS AT URBANA-CHAMPAIGN
URBANA, ILLINOIS 61801

UNCLASSIFIED
SECURITY CLASSIFICATION OF THIS PAGE

ADA183718

REPORT DOCUMENTATION PAGE

1a. REPORT SECURITY CLASSIFICATION UNCLASSIFIED	1b. RESTRICTIVE MARKINGS
2a. SECURITY CLASSIFICATION AUTHORITY	3 DISTRIBUTION/AVAILABILITY OF REPORT Distribution Unlimited
2b. DECLASSIFICATION/DOWNGRADING SCHEDULE	
4. PERFORMING ORGANIZATION REPORT NUMBER(S) UILU-ENG-87-2543; EMC 87-2	5. MONITORING ORGANIZATION REPORT NUMBER(S)
6a. NAME OF PERFORMING ORGANIZATION Electromagnetic Communication Laboratory 6b. OFFICE SYMBOL (If applicable)	7a. NAME OF MONITORING ORGANIZATION Office of Naval Research
6c. ADDRESS (City, State, and ZIP Code) Department of Elec. and Computer Engineering University of Illinois Urbana, Illinois 61801	7b. ADDRESS (City, State, and ZIP Code) John W. Michalski Department of Navy, Office of Naval Research Federal Bldg., Rm 286, 536 S. Clark St. Chicago, IL 60605
8a. NAME OF FUNDING/SPONSORING ORGANIZATION Office of Naval Research 8b. OFFICE SYMBOL (If applicable)	9. PROCUREMENT INSTRUMENT IDENTIFICATION NUMBER N00014-85-K-0619
8c. ADDRESS (City, State, and ZIP Code) Department of the Navy, Office of Naval Res. 800 N. Quincy St. Arlington, VA 22217	10. SOURCE OF FUNDING NUMBERS PROGRAM ELEMENT NO. / PROJECT NO. 410 / TASK NO. / WORK UNIT ACCESSION NO.

11 TITLE (Include Security Classification)
SCATTERING PARAMETER TRANSIENT ANALYSIS OF TRANSMISSION LINES LOADED WITH NONLINEAR TERMINATIONS

12 PERSONAL AUTHOR(S)
J. E. Schutt-Aine and R. Mittra

13a. TYPE OF REPORT	13b. TIME COVERED	14. DATE OF REPORT (Year, Month, Day)	15. PAGE COUNT
Technical	FROM _____ TO _____	March 1987	33

16 SUPPLEMENTARY NOTATION

17 COSATI CODES			18. SUBJECT TERMS (Continue on reverse if necessary and identify by block number)
FIELD	GROUP	SUB-GROUP	Scattering parameters; Flow-graph representations; Green's function; Newton-Rephson algorithm; Backward Euler algorithm; Boundary conditions; Frequency (see over)

19 ABSTRACT (Continue on reverse if necessary and identify by block number)

This work presents a new approach for the time-domain simulation of transients on a dispersive and lossy transmission line terminated with active devices. The method combines the scattering matrix of an arbitrary line and the nonlinear causal impedance functions at the load to derive a closed-form algorithm for the signal at the near and far ends.

The problems of line losses, dispersion and nonlinearities are first investigated. A time-domain formulation is then proposed using the scattering matrix representation. The algorithm assumes that dispersion and loss models for the transmission lines are available and that the frequency dependence is known. Large-signal equivalent circuits for the terminations are assumed to be given. Experimental and computer simulated results are compared for the lossless dispersionless case, and the effects of losses and dispersion are predicted.

20. DISTRIBUTION/AVAILABILITY OF ABSTRACT	21 ABSTRACT SECURITY CLASSIFICATION
☒ UNCLASSIFIED/UNLIMITED ☒ SAME AS RPT. ☐ DTIC USERS	Unclassified
22a NAME OF RESPONSIBLE INDIVIDUAL Raj Mittra	22b TELEPHONE (Include Area Code) 217-333-1202 / 22c OFFICE SYMBOL

DD FORM 1473, 84 MAR — 83 APR edition may be used until exhausted. All other editions are obsolete.

SECURITY CLASSIFICATION OF THIS PAGE
UNCLASSIFIED

Block #18 (cont.)

characterization; Propagation characteristics.

UILU-ENG-87-2543

Electromagnetic Communication Laboratory Report No. 87-2

SCATTERING PARAMETER TRANSIENT ANALYSIS OF TRANSMISSION LINES LOADED WITH NONLINEAR TERMINATIONS

by

J. E. Schutt-Aine
R. Mittra

Technical Report

March 1987

Supported by

Department of the Navy
Office of Naval Research
Contract No. N00014-85-K0619

Electromagnetic Communication Laboratory
Department of Electrical and Computer Engineering
University of Illinois at Urbana-Champaign
Urbana, Illinois 61801

SCATTERING PARAMETER TRANSIENT ANALYSIS OF TRANSMISSION LINES LOADED WITH NONLINEAR TERMINATIONS

Abstract

This work presents a new approach for the time-domain simulation of transients on a dispersive and lossy transmission line terminated with active devices. The method combines the scattering matrix of an arbitrary line and the nonlinear causal impedance functions at the load to derive a closed-form algorithm for the signal at the near and far ends.

The problems of line losses, dispersion and nonlinearities are first investigated. A time-domain formulation is then proposed using the scattering matrix representation. The algorithm assumes that dispersion and loss models for the transmission lines are available and that the frequency dependence is known. Large-signal equivalent circuits for the terminations are assumed to be given. Experimental and computer simulated results are compared for the lossless dispersionless case, and the effects of losses and dispersion are predicted.

TABLE OF CONTENTS

		Page
I.	INTRODUCTION	1
II.	FORMULATION	3
III.	SCATTERING PARAMETER FORMULATION	6
IV.	MODELS FOR TERMINATIONS AND DEVICES	15
V.	APPLICATIONS AND PRACTICAL CONSIDERATIONS	20
VI.	CONCLUSION	25
	REFERENCES	26

LIST OF FIGURES

Page

Figure 1. Transmission line with nonlinear terminations and source generator. 4

Figure 2. Transmission line and frequency domain flow-graph representation using scattering parameters. 7

Figure 3. Time-domain circuit and flow-graph representation of arbitrary transmission line (TL) with nonlinear terminations at time t. The sign * indicates a convolution between time-domain scattering parameters and the independent voltage waves a_1 and a_2 as per Equations (14) and (15) 9

Figure 4. Equivalent flow-graph representation of arbitrary transmission line with nonlinear time-varying terminations at time t. The history of the network is included via the memory variables $M_1(t)$ and $M_2(t)$. Note that this representation involves only multiplications in the time domain. 12

Figure 5. Linear capacitor and equivalent time-domain Backward-Euler representation 17

Figure 6. Geometrical and circuit interpretation of the Newton-Raphson algorithm at the k^{th} iteration 18

Figure 7. Comparison of theoretical (plots) and experimental (photographs) simulations for a stripline structure terminated with ALS inverters at near (left) and far (right) ends. The line length is 50 inches. The low-frequency characteristics are $Z_o = 73\Omega$ and $v = 0.169/ns$. Pulse width is 160 ns; rise and fall times are 4 ns. 21

Figure 8. Comparisons of simulated waveforms for a lossless (solid line) and lossy (dashed line) microstrip line with 50Ω at the near end and open at the far end. Line characteristics: length = 25 inches, low-frequency characteristic impedance : $Z_o = 60\Omega$ with loss characteristics : $R = 50\Omega/(m\text{-}\sqrt{2\pi GHz})$, $G = 0.02mhos/m$. Pulse characteristics : width = 20ns, rise and fall times : 4ns. In both cases, the dispersion model is that of [3] 23

I. INTRODUCTION

In today's many applications of integrated circuits and printed circuit boards, transmission lines and interconnections play an instrumental role at virtually every level of integration. With the design of fast devices having switching times in the picosecond range, transmitting data at high megabaud rates has become very commonplace in modern digital computers and switching networks used for telecommunication. Signal delays and rise times are more and more limited by interconnection lengths rather than by device speed and represent a potential obstacle to the ultimate scaling on VLSI technolgy. In recent years, modeling interconnections has become a major focus of interest in the implementation of digital and microwave circuits. Shorter rise and fall times as well as higher frequency signals have compelled most transmission lines to operate within ranges where dispersion is no longer negligible. Skin effect and losses contribute to signal corruption leading to waveform attenuation and a reduction of the effective dimensions. In wafer scale integration, these losses can become very significant and may lead to an RC type behavior of the lines. Finally, in the case of multiconductor lines, cross-coupling between neighboring lines may increase the level of distortion in excited lines which can initiate false signals in non-excited lines.

The implementation of a high-density compatible packaging scheme is essential for the design of high-speed digital systems such as gallium arsenide integrated circuits, for microwave or digital applications, printed circuit boards, chip carriers, and modeling of these networks represents the first step toward implementing reliable design guidelines. A complete CAD tool for studying these effects would require a frequency domain characterization of the transmission line with higher-order modes included to account for dispersion. Numerous authors have investigated the properties of microstrip lines at high frequencies and derived expressions

relating the propagation characteristics to frequency [1]-[10]. Full-wave and simplified models have been proposed to describe these effects and derive the frequency dependence of the characteristic impedance and the propagation constant. Other geometries such as stripline, buried microstrip or coplanar have thus far received less attention but obey the same restrictions imposed on the electrical performance of microstrip at microwave frequencies.

Of equal importance is the analysis of a high-speed or high-frequency signal propagating on a dispersive and lossy transmission line. Such an analysis requires a complete and accurate frequency characterization of the structure of interest and, for practicality, must implement the nonlinear and time-changing behaviors of the terminations, which are transistors, logic gates or other types of active devices. Several investigators have attempted to set up analytical models describing wave propagation in such systems. Solutions for lossless lines with arbitrary terminations were obtained by Mohammadian *et al.* [12] using a forward and backward wave approach. Veghte and Balanis [13] have analyzed the distortion of a pulse due to dispersion along a microstrip transmission line. Djordjevic *et al.* [11] used a complementary network approach to simulate the time-domain transient on a multiconductor array with nonlinear terminations. However, exact closed-form solutions that combine losses and nonlinear terminations have not been made available as yet.

In this study, a combined frequency-domain time-domain approach is used to formulate the propagation equations on a dispersive and lossy line with nonlinear behavior at the terminations. The method uses the scattering parameters of the transmission line to derive a closed-form algorithm for the propagation of an arbitrary signal in the time domain. In the lossless case, the solution reduces to very simple expressions which greatly increase computational efficiency.

II. FORMULATION

Consider an arbitrary transmission line with arbitrary loads at both ends (see Fig. 1). The differential equations relating the voltage V and the current I along the line are expressed by

$$-\frac{\partial V}{\partial x} = L_o \frac{\partial I}{\partial t} + R_o I \tag{1a}$$

$$-\frac{\partial I}{\partial x} = C_o \frac{\partial V}{\partial t} + G_o V \tag{1b}$$

where L_o , C_o, R_o and G_o are the inductance, capacitance, resistance, and conductance per unit length, respectively, and must be regarded as functions of frequency to preserve generality. The solutions for time-harmonic excitation are usually written in the frequency domain as ($\omega = 2\pi f$ is angular frequency)

$$V(\omega,x) = Ae^{-\beta x} + Be^{+\beta x} \tag{2a}$$

$$I(\omega,x) = \frac{1}{Z_o}\left[Ae^{-\beta x} - Be^{+\beta x}\right] \tag{2b}$$

where

$$\beta = \sqrt{(R_o + j\omega L_o)(G_o + j\omega C_o)} \qquad Z_o = \sqrt{\frac{R_o + j\omega L_o}{G_o + j\omega C_o}} \tag{3}$$

β and Z_o are complex leading to an attenuation of the signal as it propagates through the medium. If the terminations are linear, (i.e., $Z_s(t)$ and $Z_L(t)$ constant with time), the coefficients **A** and **B** can be determined by matching boundary conditions at **x=0** and **x=l**; next, an inverse Fourier transform approach can be used to solve for the time-domain solution. On the other hand, if the terminations are nonlinear or time-changing, then the boundary conditions must be formulated in

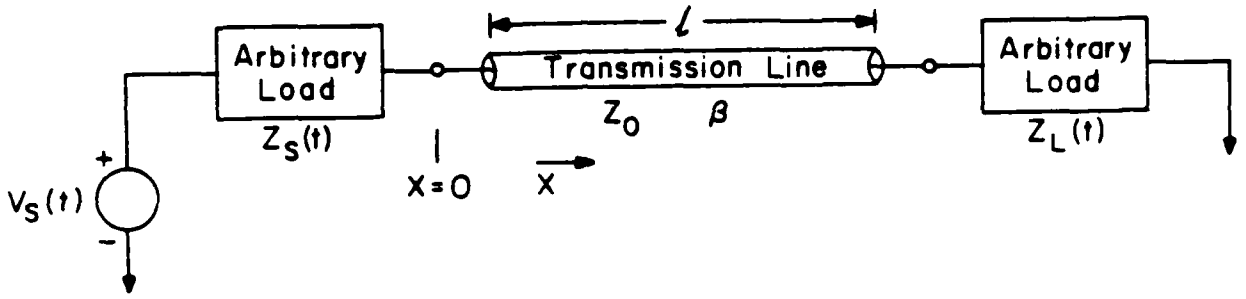

Figure 1. Transmission line with nonlinear terminations and source generator.

the time domain as

$$v_s(t) = V(t,0)+Z_s(t)\, I(t,0) \tag{4}$$

$$Z_L(t)\, I(t,l) = V(t,l) \tag{5}$$

where $v_s(t)$ is the source voltage. $Z_s(t)$ and $Z_L(t)$ indicate the time variations of the source and load terminations, respectively. For any time greater than t, $Z_s(t)$ and $Z_L(t)$ are not known since they depend on the voltage and current solutions at time t. In fact, the evaluation of $Z_s(t)$ and $Z_L(t)$ may involve several iterations consisting of solving the propagation equations with trial values until convergence to the true impedance values. Transforming conditions (4) and (5) into the frequency domain is inappropriate and a time-domain formulation is thus necessary. Likewise, (2) and (3) cannot be conveniently inverted into the time domain in a closed-form and constrained to satisfy (4) and (5). This limitation arises not only because of the dispersive and frequency-dependent characteristics of the line, but also because the evaluation of the coefficients **A** and **B** requires an *a priori* knowledge of the time-dependent load functions. A formulation in which the causality of the boundary conditions is implied thus becomes necessary. The use of scattering parameters allows one to define the properties of the transmission line independently from those of the terminations; consequently, by properly combining load and line relations, a closed-form algorithm for the solutions can be derived.

III. SCATTERING PARAMETER FORMULATION

Any linear two-port network can be described as a set of scattering parameters or (S-parameters) which relate incident and reflected voltage waves. These waves are variables which depend on the total voltages and currents at the two-port. If ideal (lossless and dispersionless) transmission lines of known characteristic (reference) impedance Z_{ref} are connected to both ports of a linear network, then the voltage waves on the reference lines (see Fig. 2) a_1, b_1, a_2, b_2 are defined as the incident and reflected waves from port 1 and port 2, respectively. The scattering parameters are then known to satisfy the frequency domain relation.

$$b_1 = \tilde{S}_{11}a_1 + \tilde{S}_{12}a_2 \tag{6}$$

$$b_2 = \tilde{S}_{21}a_1 + \tilde{S}_{22}a_2 \tag{7}$$

$\tilde{S}_{11}$ and $\tilde{S}_{22}$ are regarded as reflection coefficients whereas $\tilde{S}_{12}$ and $\tilde{S}_{21}$ are the transmission scattering coefficients of the network. The total voltages in ports 1 and 2 are respectively given by

$$V_1 = a_1 + b_1 \tag{8}$$

$$V_2 = a_2 + b_2 \tag{9}$$

and the expressions for the currents are

$$I_1 = \frac{a_1}{Z_{ref}} - \frac{b_1}{Z_{ref}} \tag{10}$$

$$I_2 = \frac{a_2}{Z_{ref}} - \frac{b_2}{Z_{ref}} \tag{11}$$

A relation between the propagation characteristics of a transmission line and the associated scattering parameters can then be easily derived. For a single mode of propagation, it can be shown that for a given transmission line

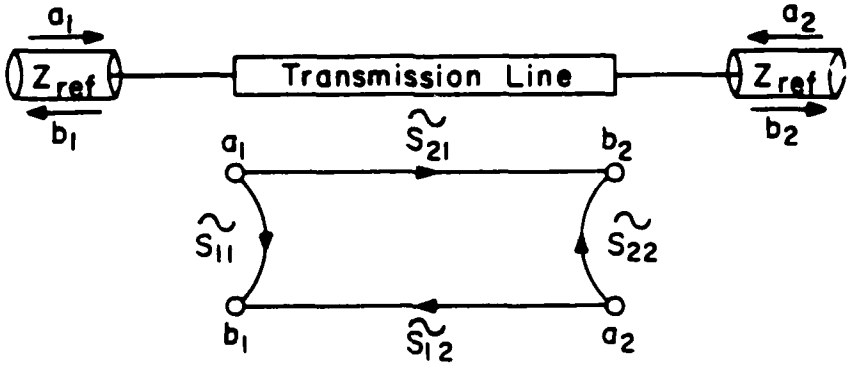

Figure 2. Transmission line and frequency domain flow-graph representation using scattering parameters.

$$\tilde{S}_{11} = \tilde{S}_{22} = \frac{(1-\rho^2)\alpha}{1-\rho^2\alpha^2} \qquad \tilde{S}_{12} = \tilde{S}_{21} = \frac{(1-\alpha^2)\rho}{1-\rho^2\alpha^2} \tag{12}$$

$$\alpha = e^{-\gamma l} \qquad \rho = \frac{Z_o(\omega)-Z_{ref}}{Z_o(\omega)+Z_{ref}} \tag{13}$$

where $\alpha(\omega)$ and $Z_o(\omega)$ account for the dispersive and lossy behaviors of the line. The scattering parameters of a transmission line depend only on its electrical characteristics and are not influenced by the source and load voltages at the terminations; however, the overall response of the system is a combination of line and termination responses and can be obtained by cascading the various sections of the network. We can then write the time-domain equations relating the voltage waves of an arbitrary line terminated with nonlinear loads (Fig 3). We get (subscripts 1 and 2 refer to near end and far end, respectively)

$$b_1(t) = S_{11}(t)*a_1(t) + S_{12}(t)*a_2(t) \tag{14}$$

$$b_2(t) = S_{21}(t)*a_1(t) + S_{22}(t)*a_2(t) \tag{15}$$

where * indicates a convolution in the time-domain. The scattering parameters $S_{11}(t)$, $S_{12}(t)$, $S_{21}(t)$, $S_{22}(t)$ are the inverse transforms of the frequency domain S-parameters and can be viewed as Green's functions associated with the time domain response of the transmission line, due to a single frequency source at the terminations. The load conditions at the near and far ends are now directly expressed in the time-domain by looking at the flow-graph representation of the system (see Fig. 3)

$$a_1(t) = \Gamma_1(t)b_1(t) + T_1(t)g_1(t) \tag{16}$$

$$a_2(t) = \Gamma_2(t)b_2(t) + T_2(t)g_2(t) \tag{17}$$

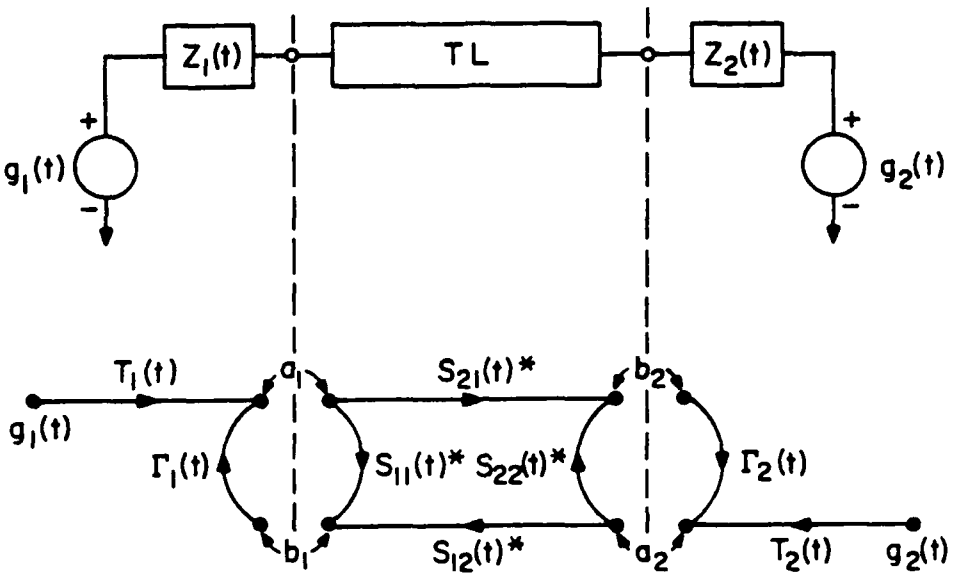

Figure 3. Time-domain circuit and flow-graph representation of arbitrary transmission line (TL) with nonlinear terminations at time t. The sign * indicates a convolution between time-domain scattering parameters and the independent voltage waves a_1 and a_2 as per Equations (14) and (15) .

in which $\Gamma_1(t), \Gamma_2(t), T_1(t), T_2(t)$ are the reflection and transmission coefficients associated with near and far ends respectively.

$$T_i(t) = \frac{Z_{ref}}{Z_i(t) + Z_{ref}} \qquad \Gamma_i(t) = \frac{Z_i(t) - Z_{ref}}{Z_i(t) + Z_{ref}} \tag{18}$$

In Eqs. (14) and (15), each of the convolutions terms can be expressed as

$$S_{ij} * a_j = \int_0^t S_{ij}(t-\tau) a_j(\tau) d\tau \tag{19}$$

Since the algorithm to be derived must be amenable to computer usage, it is desirable to discretize (19) as

$$S_{ij}(t) = \sum_{\tau=1}^{t} S_{ij}(t-\tau) a_j(\tau)\, \Delta\tau \tag{20}$$

$$S_{ij}(t) = S_{ij}(0)\, a_j(t)\Delta\tau + \sum_{\tau=1}^{t-1} S_{ij}(t-\tau)\, a_j(\tau)\Delta\tau$$

or

$$S_{ij}(t) = S'_{ij}(0) a_j(t) + H_{ij}(t) \tag{21}$$

where $\Delta\tau$ is the time step and $S'_{ij}(0) = S_{ij}(0)\Delta\tau$. $H_{ij}(t) = \sum_{\tau=1}^{t-1} S_{ij}(t-\tau)\, a_j(\tau)\Delta\tau$ represents the history of the line and depends on information up to time t-1. Causality insures that the a_j's are known for $\tau < t$, which allows the use of this information for the determination of the a_j's at $\tau = t$. We first substitute (21) into (14) and (15) and obtain

$$b_1(t) = S'_{11}(0)\, a_1(t) + S'_{12}(0)\, a_2(t) + H_{11}(t) + H_{12}(t) \tag{22}$$

$$b_2(t) = S'_{21}(0)\, a_1(t) + S'_{22}(0)\, a_2(t) + H_{21}(t) + H_{22}(t) \tag{23}$$

Combining the above equations with those for the forward waves (16) and (17), one gets

$$a_1(t) = \frac{[1 - \Gamma_2(t)S'_{22}(0)]\,[T_1(t)g_1(t) + \Gamma_1(t)M_1(t)]}{\Delta(t)} + \frac{\Gamma_1(t)S'_{12}(0)[T_2(t)g_2(t) + \Gamma_2(t)M_2(t)]}{\Delta(t)} \tag{24}$$

$$a_2(t) = \frac{[1 - \Gamma_1(t)S'_{11}(0)]\,[T_2(t)g_2(t) + \Gamma_2(t)M_2(t)]}{\Delta(t)} + \frac{\Gamma_2(t)S'_{21}(0)[T_1(t)g_1(t) + \Gamma_1(t)M_1(t)]}{\Delta(t)} \tag{25}$$

$$\Delta(t) = [1 - \Gamma_1(t)S'_{11}(0)][1 - \Gamma_2 S'_{22}(0)] - \Gamma_1(t)S'_{12}(0)\Gamma_2(t)S'_{21}(0) \tag{26}$$

where $M_1(t) = H_{11}(t) + H_{12}(t)$ and $M_2(t) = H_{21}(t) + H_{22}(t)$. $b_1(t)$ and $b_2(t)$ are recovered using (22) and (23), and the total voltages at ports 1 and 2, by using (8) and (9). Figure 4 shows the flow graph representation for the transmission line at time t in which the memory of the network has been included in the terms $M_1(t)$ and $M_2(t)$. The independent terms are $g_1(t)$ and $g_2(t)$. $M_1(t)$ and $M_2(t)$ are also independent and contain the information pertinent to the history of the line. Numerical considerations are of importance for the simulation since they determine the speed of the computations involved. Expressions (24)-(26) can be further reduced by observing that for transmission lines with nonzero length, $S'_{12}(0)$ and $S'_{21}(0)$ must vanish since a finite duration is required for an arbitrary signal to propagate through the line. The above relations then become

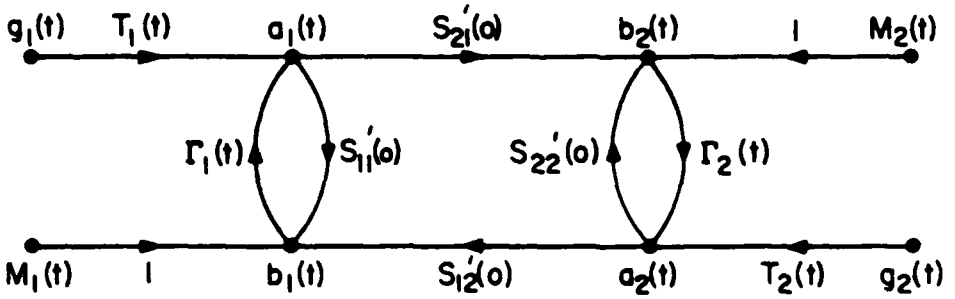

Figure 4. Equivalent flow-graph representation of arbitrary transmission line with nonlinear time-varying terminations at time t. The history of the network is included via the memory variables $M_1(t)$ and $M_2(t)$. Note that this representation involves only multiplications in the time domain.

$$a_1(t) = \frac{[1 - \Gamma_2(t)S'_{22}(0)][T_1(t)g_1(t) + \gamma_1(t)]}{\Delta(t)} \tag{27a}$$

$$a_2(t) = \frac{[1 - \Gamma_1(t)S'_{11}(0)][T_2(t)g_2(t) + \gamma_2(t)]}{\Delta(t)} \tag{27a}$$

$$b_1(t) = S'_{11}(0)a_1(t) + M_1(t) \tag{27c}$$

$$b_2(t) = S'_{22}(0)a_2(t) + M_2(t) \tag{27d}$$

with

$$\Delta(t) = [1 - \Gamma_1(t)S'_{11}(0)][1 - \Gamma_2(t)S'_{22}(0)] \tag{28}$$

Computational limitations in these expressions are essentially determined by $M_1(t)$ and $M_2(t)$ which contain the history of the network and involve the voltage wave solutions from previous time steps. In the case where losses and dispersion are neglected, the frequency domain scattering parameters associated with the transmission line become

$$\tilde{S}_{11}(\omega) = \tilde{S}_{22}(\omega) = \frac{(1 - e^{-2\frac{j\omega l}{v}})\rho}{1 - \rho^2 e^{-2\frac{j\omega l}{v}}} \tag{29}$$

$$\tilde{S}_{12}(\omega) = \tilde{S}_{21}(\omega) = \frac{(1 - \rho^2)\, e^{-\frac{j\omega l}{v}}}{1 - \rho^2 e^{-2\frac{j\omega l}{v}}} \tag{30}$$

where

$$\rho = \frac{Z_o - Z_{ref}}{Z_o + Z_{ref}} \tag{31}$$

Since Z_o, the characteristic impedance of the line is constant with time, and since

Z_{ref} the reference impedance is arbitrary, one can choose $Z_{ref}=Z_o$ which leads to $\rho = 0$ and

$$\tilde{S}_{11}(\omega) = \tilde{S}_{22}(\omega) = 0 \tag{32}$$

$$\tilde{S}_{12}(\omega) = S_{21}(\omega) = e^{-\frac{j\omega l}{v}} \tag{33}$$

Therefore, the time domain Green's functions associated with the scattering parameters are

$$S_{11}(t) = S_{22}(t) = 0 \tag{34}$$

$$S_{12}(t) = S_{21}(t) = \delta(t-\frac{l}{v}) \tag{35}$$

$$M_1(t) = a_2(t-l/v) \tag{36}$$

$$M_2(t) = a_1(t-l/v) \tag{37}$$

$$\Delta(t) = 1 \tag{38}$$

We then obtain simple expressions for the forward and backward waves

$$a_1(t) = T_1(t)g_1(t) + \Gamma_1(t)a_2(t-l/v) \tag{39}$$

$$a_2(t) = T_2(t)g_2(t) + \Gamma_2(t)a_1(t-l/v) \tag{40}$$

$$b_1(t) = a_2(t-l/v) \tag{41}$$

$$b_2(t) = a_1(t-l/v) \tag{42}$$

The advantage of the above expressions lies in their computational efficiency since only a search is involved in the evaluation of the history of the network and no summations of previously calculated terms are needed.

IV. MODELS FOR TERMINATIONS AND DEVICES

Thus far, this study concentrated on simulating the time-domain transient response for arbitrary transmission lines terminated with nonlinear devices. In this section, we examine the nature of the terminations and the manner in which they are to be represented in a form consistent with the relations derived. Several techniques are available that convert reactive elements and nonlinear devices to time-varying causal resistances as well as voltage or current sources. We briefly overview two of these techniques, namely, the Backward Euler scheme and the Newton-Raphson (NR) algorithm. A more detailed development can be found in [14]. Since formulation and solution are in the time domain, every element must have an equivalent network in the time domain. The Backward Euler algorithm is a numerical integration scheme and its use in representing reactive elements in the time domain is illustrated below. Consider a capacitor **C**, with a current voltage relation given by

$$I = C\frac{dV}{dt} \tag{43}$$

If we discretize the time variable by choosing a time step **h**, then the voltage V_{n+1} at time $t_{n+1} = (n+1)h$ can be approximated in terms of variables at $t = nh$ as

$$V_{n+1} = V_n + hV'_{n+1} \tag{44}$$

where the superscript ' indicates a derivative with respect to time. Making use of (43), we get

$$I_{n+1} = \frac{C}{h}V_{n+1} - \frac{C}{h}V_n \tag{45}$$

Equation (45) can be represented by the equivalent linear one-port model at time

$t_{n+1} = (n+1)h$ (see Fig. 5) with conductance $G = \frac{C}{h}$ and current source $J_n = \frac{C}{h}V_n$. Such transformations can be applied to inductances as well. The efficiency of the method depends on a proper choice of the time step which determines the stability of the numerical solution. Other techniques of numerical integration can be used if greater stability is desired [14].

Nonlinear elements such as diodes and transistors must be reduced to equivalent networks with only linear elements at time t. If the nonlinear current voltage relation for these elements is known, then an iterative scheme such as the Newton-Raphson algorithm can be used to seek a solution. The circuit representation of the Newton-Raphson technique is illustrated in Figure 6. At a particular time, a guess value for the voltage is chosen to which a current is associated via the I-V relations that determine the operating point Q. The next guess is then related to the previous one by

$$I_{k+1} = I_k - \left|\frac{dV}{dI}\right|^{-1} I_k \tag{46}$$

At each iteration step, the resulting equivalent circuit is composed of a linear conductance of value $G_k = dI/dV$ at V_k and a current source with value given by $J_k = I(V_k) - G_k V_k$. Solving the combined transmission line, Newton-Raphson equivalent circuit problem at each iteration step will lead to the actual representation of the termination at time t.

Once linearization and discretization are performed, time domain values are available for the terminations' equivalent impedances or generators. These expressions are causal, since their values at any time t depend on the history of the network which renders impossible an *a priori* knowledge of the time variations of the

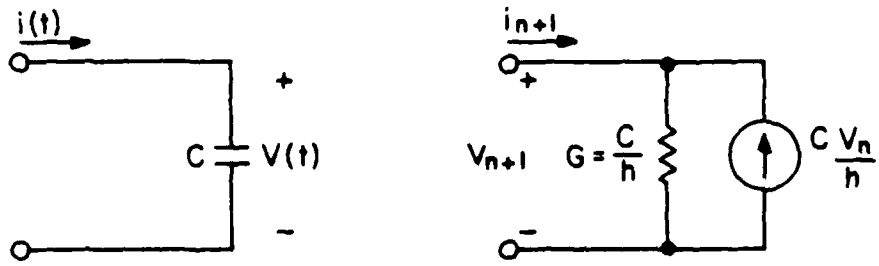

Figure 5. Linear capacitor and equivalent time-domain Backward-Euler representation.

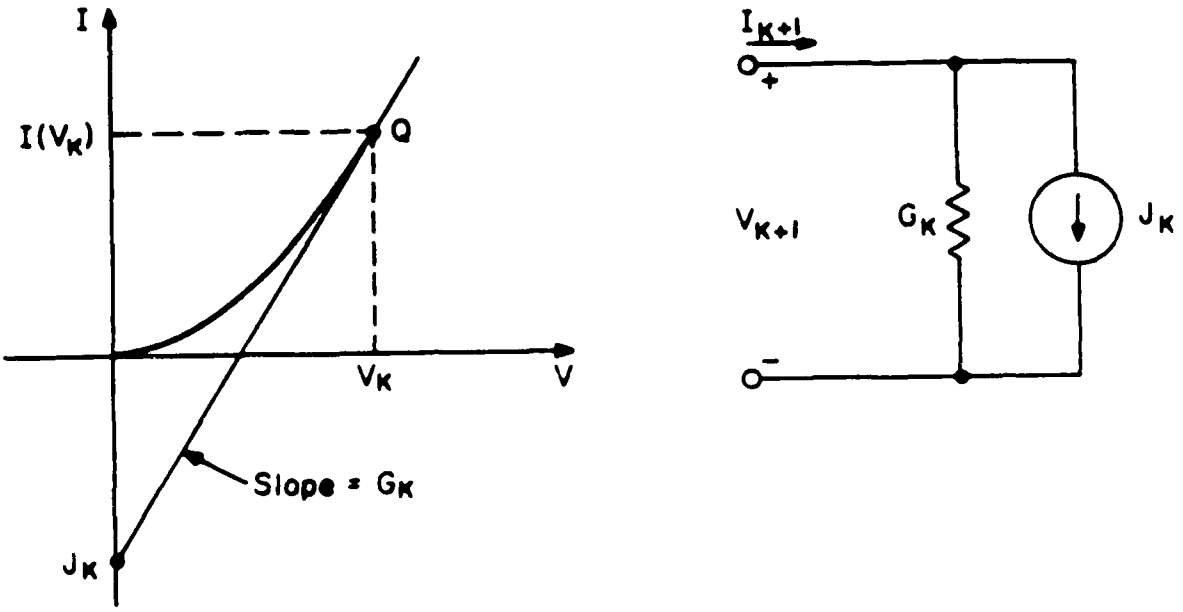

Figure 6. Geometrical and circuit interpretation of the Newton-Raphson algorithm at the k^{th} iteration.

termination impedance. Nonlinear complex elements can be handled by first using the NR scheme for linearization at a given time then stepping in the time domain while replacing linear complex elements by time-varying resistances and generators.

V. APPLICATIONS AND PRACTICAL CONSIDERATIONS

Many applications in microwave and digital communications require the use of transmission lines terminated with nonlinear devices. Distortion and noise arise when the terminations are not matched to the line impedance. Moreover, if losses and dispersion are present in the line, attenuation and delay come into account. The combination of these effects needs to be modeled and simulated on a reliable CAD tool. The above algorithms were used to predict signals at the near and far ends of a 73 Ω stripline structure terminated with ALS inverters. The length of the line was 50 inches. The pulse characteristics are summarized in Figure 7. Results were compared with experimental measurements and good agreement indicated the validity of the assumptions.

Equations (27) were used to predict the waveforms on a microstrip line having dispersive and lossy characteristics. Predicted distortion waveforms, line parameters and simulation data are summarized in Figure 8. The dispersion model of Bhartia and Pramanick [3] was used. This model provided the frequency domain data with a frequency-dependent effective dielectric constant and characteristic impedance. A $\sqrt{f}$ behavior was assumed for the resistance per unit length to model the skin effect. Waveform attenuation as well as rise and fall time degradation can be observed from the simulations. Wafer scale integration and VLSI interconnections that possess higher loss parameters [15] should be expected to present a higher level of signal degradation.

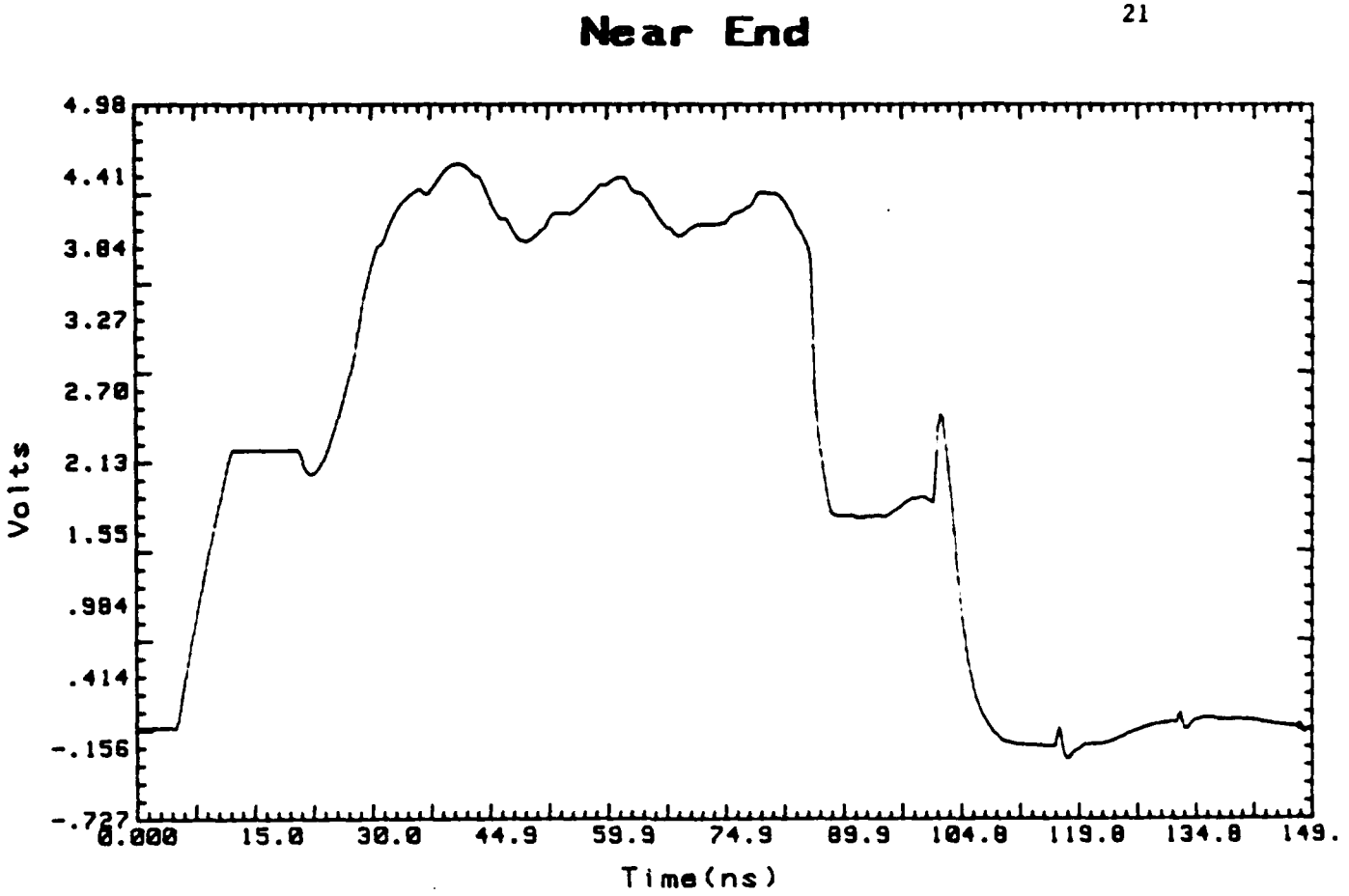

Figure 7. Comparison of theoretical (plots) and experimental (photographs) simulations for a stripline structure terminated with ALS inverters at near (left) and far (right) ends. The line length is 50 inches. The low-frequency characteristics are Z_o = 73Ω and v = 0.169/ns. Pulse width is 160 ns; rise and fall times are 4 ns.

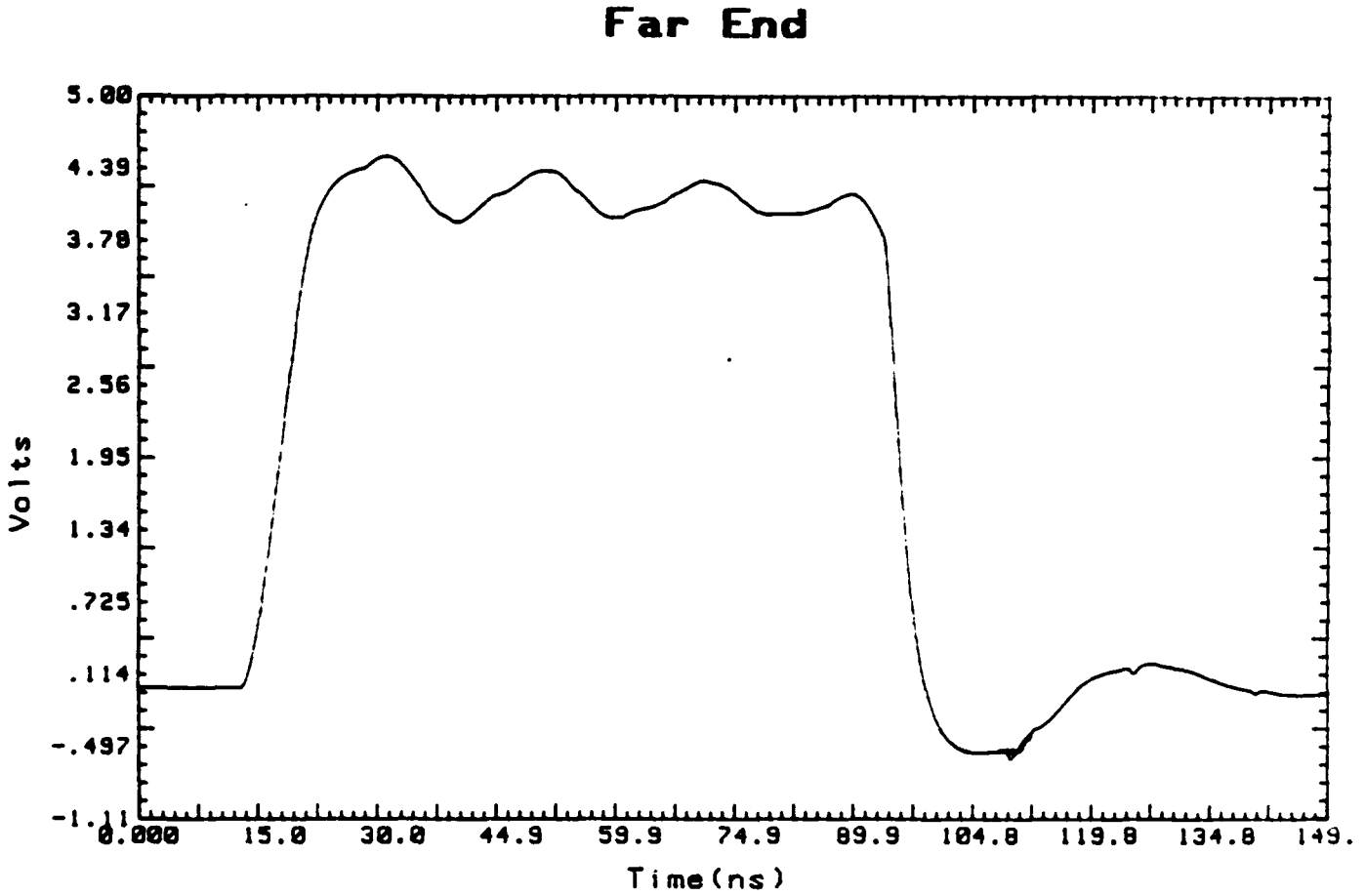
Far End
5.00
4.39
3.78
3.17
2.56
1.95
1.34
.725
.114
-.497
-1.11
Volts
0.000
15.0
30.0
44.9
59.9
74.9
89.9
104.8
119.8
134.8
149.
Time(ns)

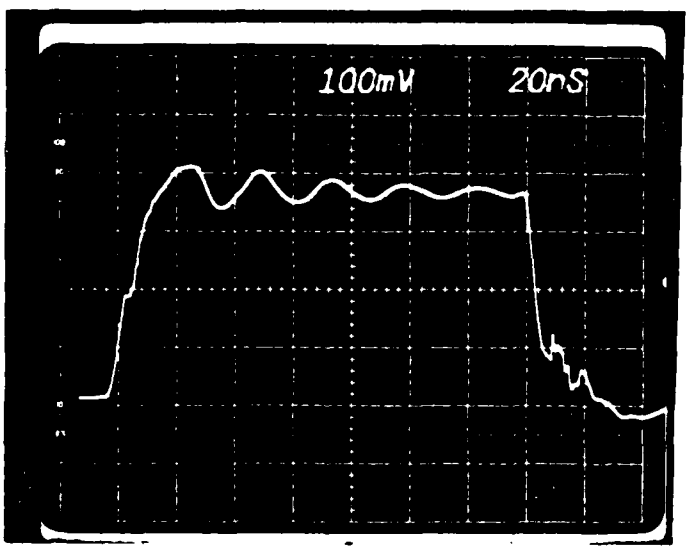
100mV
20nS

Figure 7. [illegible]

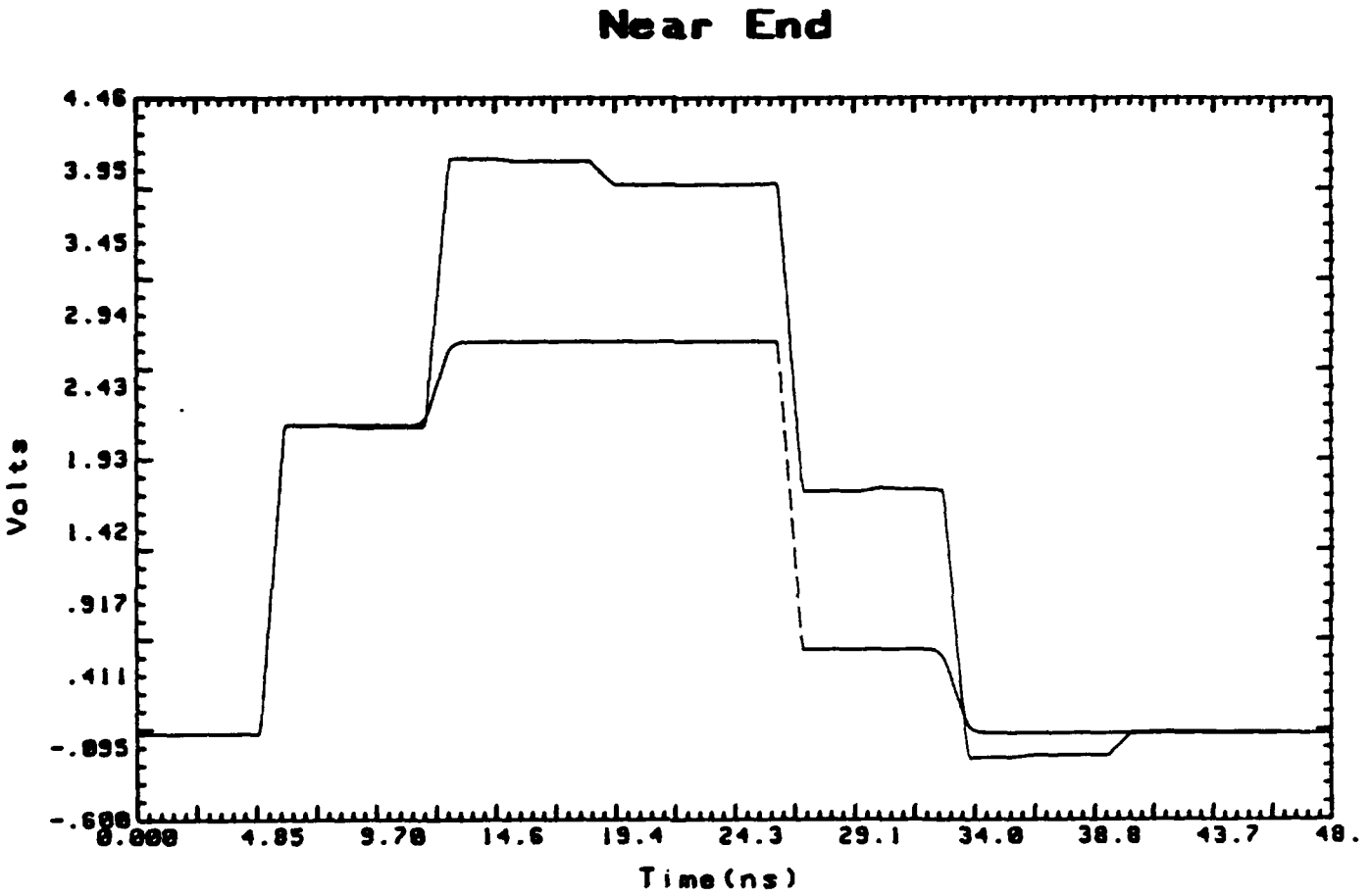

Figure 8. Comparisons of simulated waveforms for a lossless (solid line) and lossy (dashed line) microstrip line with 50Ω at the near end and open at the far end. Line characteristics: length = 25 inches, low-frequency characteristic impedance : $Z_0 = 60\Omega$ with loss characteristics : $R = 50\Omega/(m - \sqrt{2\pi GHz})$, $G = 0.02$mhos/m. Pulse characteristics : width = 20ns, rise and fall times : 4ns. In both cases, the dispersion model is that of [3].

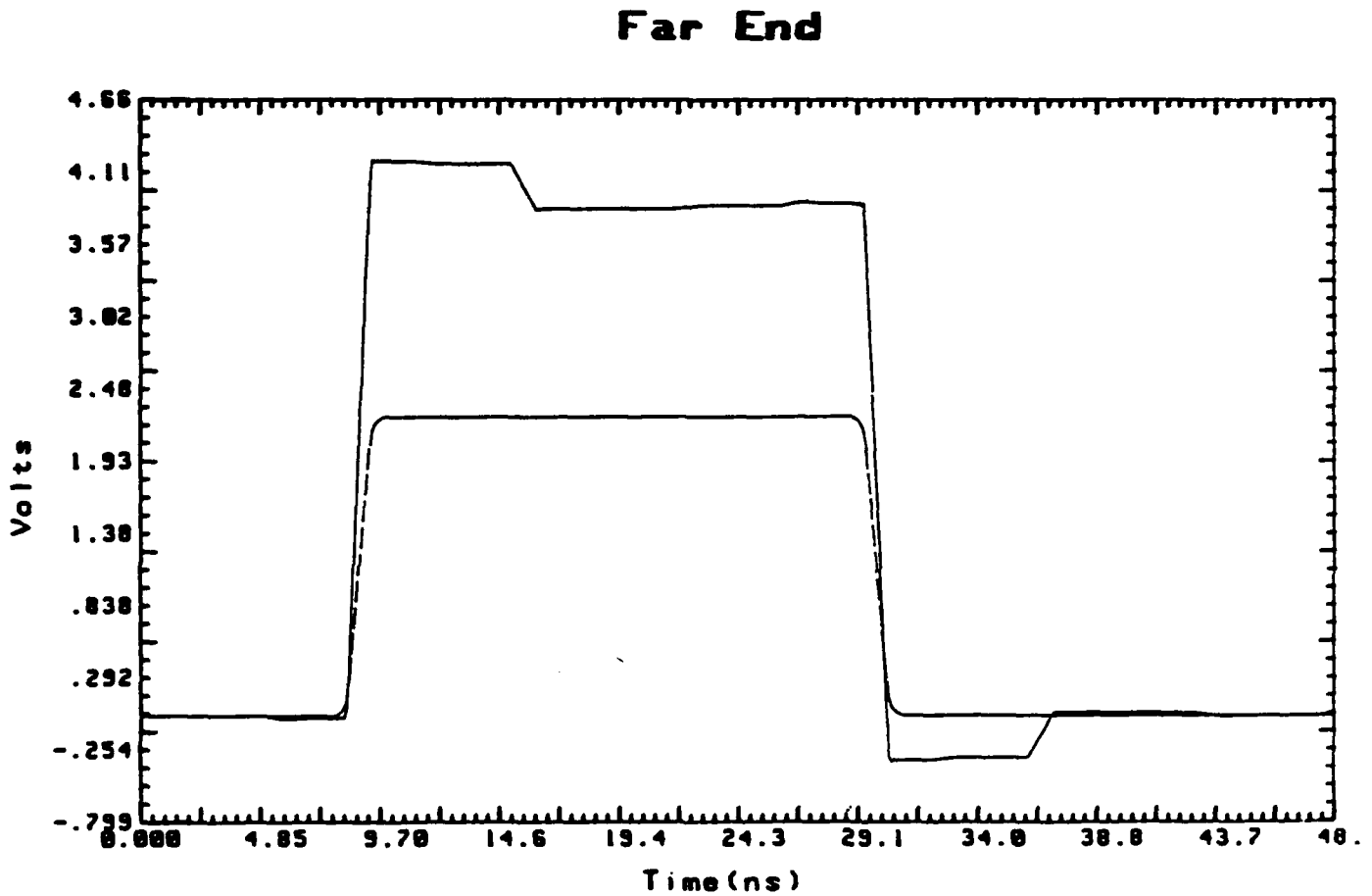

Figure 8. (Continued)

VI. CONCLUSION

This study explored some important aspects of interconnections for digital and microwave applications. The problems of losses, dispersion and load non-linearities were analyzed. A closed-form algorithm was derived for the simulation of an arbitrary time-domain signal on a structure having all the above properties. The algorithm assumed that the frequency-dependent characteristics of the line were available as well as large-signal models for the terminations. Future work includes the derivation of a suitable loss and dispersion model and the extension of the algorithm for modeling n-line multiconductor systems.

REFERENCES

[1] W. J. Getsinger, "Microstrip Dispersion Model," *IEEE Trans. Microwave Theory Tech.*, vol. MTT-21, pp. 34-39, January 1973.

[2] W. J. Getsinger, "Measurement and Modeling of the Apparent Characteristic Impedance of Microstrip," *IEEE Trans. Microwave Theory Tech.*, vol. MTT-31, pp. 624-632, August 1983.

[3] P. Bhartia and P. Pramanick, " New Microstrip Dispersion Model," *IEEE Trans. Microwave Theory Tech.*, vol.,MTT-32, pp. 1379-1384, October 1984.

[4] H. J. Carlin, " A Simplified Circuit Model for Microstrip," *IEEE Trans. Microwave Theory Tech.*, vol. MTT-21, pp. 589-591, September 1973.

[5] E. J. Denlinger, "A Frequency Dependent Solution for Microstrip Transmission Lines," *IEEE Trans. Microwave Theory Tech.*, vol. MTT, pp. 30-39, January 1971.

[6] T. Itoh and R. Mittra, "Spectral-Domain Approach for Calculating the Dispersion Characteristics of Microstrip Lines," *IEEE Trans. Microwave Theory Tech.*, vol. MTT-21, pp. 496-499, July 1973.

[7 R. Mittra and T. Itoh, " New Technique for the Analysis of the Dispersion Characteristics of Microstrip Lines," *IEEE Trans. Microwave Theory Tech.*, vol. MTT-19, pp. 47-56, January 1971.

[8] E. F. Kuester and D. C. Chang, "Theory of Dispersion in Microstrip of Arbitrary Width," *IEEE Trans. Microwave Theory Tech.*, vol. MTT-28, pp. 259-265, March 1980.

[9] M. Hashimoto, "A Rigorous Solution for Dispersive Microstrip," *IEEE Trans.*

END

9-87

DTIC